

# Sustainable Design and Numerical Analysis of Auditorium Air Distribution Systems: Equal Friction Method and CFD Insights.

Ryne P M<sup>1\*</sup>, Dr. P Sridharan<sup>2†</sup>, Dr S Christopher Ezhil Singh<sup>3†</sup>

<sup>1</sup> Research Scholar APJKTU, Vimal Jyothi Engineering College, Kannur, India -670632,

<sup>2,3</sup> Professor, Vimal Jyothi Engineering College, Kannur, India -670632

\* Corresponding author E-mail : [rynepm7@gmail.com](mailto:rynepm7@gmail.com),

Contributing authors: [sridharanp@vjec.ac.in](mailto:sridharanp@vjec.ac.in); [christopher0420@vjec.ac.in](mailto:christopher0420@vjec.ac.in)

†These authors contributed equally to this work.

## Abstract

Heating, Ventilation, and Air Conditioning (HVAC) systems play a vital role in maintaining indoor environmental quality, occupant health, and thermal comfort in large public spaces such as auditoriums. However, inadequately designed duct networks often result in uneven airflow, increased energy consumption, and higher operational costs, thereby contributing to greater environmental impact. In this study, cooling load calculations were performed based on occupancy and seating arrangements, followed by diffuser placement and duct network design. Duct sizing was carried out using the Equal Friction Method, and pressure variations across ducts with different aspect ratios were numerically analysed. Three-dimensional models of the duct system were developed using SolidWorks, and Computational Fluid Dynamics (CFD) simulations using Wizard software were conducted to evaluate airflow distribution, velocity profiles, and pressure characteristics. The results show that duct sizing optimized through the Equal Friction Method produces uniform air distribution without the need for additional flow-regulating devices, thereby reducing pressure losses and improving energy efficiency. This leads to enhanced HVAC system performance and improved indoor air quality. This study uniquely integrates the Equal Friction Method with CFD analysis by using the analytical method for initial duct sizing and the CFD model to validate and optimize airflow distribution and thermal comfort within the auditorium. This combined approach advances existing HVAC design practices by providing a more accurate, cost-effective, and performance-oriented framework compared to other methods, while also supporting sustainable and environmentally responsible building design.

**Keywords:** HVAC, Duct system, Auditorium, CFD simulation, Equal Friction Method

## 1. Introduction

In centralized air-conditioning systems, conditioned air is generated in a central plant room and distributed to occupied spaces through a network of air ducts. The quality and quantity of supplied air are therefore critical parameters in ensuring thermal comfort, indoor air quality, and occupant satisfaction in large commercial environments such as shopping malls and auditoriums. HVAC duct system optimization is commonly carried out by following established duct design procedures to determine appropriate duct dimensions, airflow rates, and velocities, followed by analytical evaluation and numerical simulation. However, when duct networks are designed without a systematic and validated methodology, the resulting airflow distribution is often non-uniform, leading to excessive air supply at certain diffusers and insufficient air delivery at others. This imbalance not only degrades thermal comfort and indoor air quality but also increases energy consumption and operational costs, thereby reducing overall system efficiency. The dimensions of the main duct and sub ducts should be accurately sized so that correct volume of air is circulated through them based on the demand (Whalley and Abdul-Ameer 2011). Experimental and computational fluid dynamics methods were adopted to analyze the inter zonal heat transfer (IZHT) at two model scales and proposed a novel cooling load calculation method for stratified air-conditioning (STRAC) systems (Wang *et al.* 2023). This is called inter zonal thermal resistance method and is based on equivalent heat transfer coefficient  $K_c$  whose value ranged from  $42.66 \text{ W/m}^2 \text{ }^\circ\text{C}$  to  $44.36 \text{ W/m}^2 \text{ }^\circ\text{C}$ . It was observed that the difference between the cooling load calculated by traditional method and newly developed method was only 4.16 % which proves the reliability of the method. This is an alternate method for calculating the cooling load of STRAC systems which is more convenient method than traditional method. Computational Fluid Dynamics (CFD) concepts were used to study the occupant comfort and enhance building performance across different seasons in a subtropical climate (Chowdhury *et al.* 2022). The thermal CFD model applied in the study incorporated advanced turbulence simulation techniques suited for

indoor airflow analysis. Indoor thermal conditions were assessed using a numerical comfort analysis approach. Findings of the simulation was that uniform temperature distribution was observed during the working hours and there was adequate improvement in energy efficiency of the building systems. The findings indicated that advanced CFD techniques serve as an effective tool for evaluating human comfort in indoor environments. Energy consumption related to ventilation and air-conditioning (VAC) was thoroughly simulated to assess the energy-saving potential of five commonly applied strategies: mechanical fresh air intake, PSD air sealing, indoor temperature settings, chiller coefficient of performance (COP), and the energy efficiency ratio (EER) of terminal units (Su and Li 2022). Energy saving operation solutions and suggestions were put forward quantitatively and specifically, which provide reference for operations to adopt effective energy saving operation measures. Variable shape of a river channel influenced by sedimentation was used to study the reduction in resistance of local elements of a duct and the effect of silty sediment and resistance within the channel was discussed. As a result of this, a reduced scale test bench was constructed using Boltzmann curve instead of traditional straight-line connection variable diameter (Gao et al. 2021). Duct layout for an auditorium was designed and analyzed the performance using CFD and the effect of pressure drop, turbulence, recirculation zone, and flow efficiency of the duct was investigated and the optimization model significantly helped to install the duct layout for the buildings (Aravinda et al. 2017). A method for optimizing the resistance reduction of variable diameters suitable for different aspect ratios and area ratios were obtained. Performance of 4-way cassette air conditioner installed to an office room was studied and compared it with wall mounted mixing ventilation system and CFD simulation was done and results indicated that air distribution performance by 4-way cassette AC is superior and more uniform than that of wall mounted system based on the air diffusion performance index (Bamodu et al. 2017). It is expected that 4-way cassette AC will perform better than typical mixing ventilation system in square room and optimizing the temperature and angle of the supply air has possible potential of saving the energy. A computer aided method for completely automating the heating,

ventilation and air conditioning duct system design process was proposed (Walunj *et al.* 2021; Liang *et al.* 2023). This method incorporated duct selection and hydraulic calculation, and introduced a rule-based divide-and-conquer method to the pipe routing design (PRD). The research assesses the practical effect of this piping design algorithm in a BIM environment using varied building scenarios. The findings showed that the proposed method is capable of meeting the design requirements of actual projects and significantly reduce the labor cost associated with HVAC design eliminating the calculation errors. Study on design and modifications of air-cooling duct using CFD analysis was conducted considering all air flow features relating to the duct system efficiency (Khakre and Wankhade 2014). This study combines theoretical and software enabled tools to provide a detailed comparative analysis of the costs and benefits involved in selecting a particular shape of duct for a prescribed situation. A method based on computational fluid dynamics was proposed to determine the pressure drop and air distribution characteristics in recuperative heat exchangers, numerical calculations were performed for a representative counter flow heat exchanger with a relatively complex structure providing a large heat exchange surface (Pacak *et al.* 2023). The verification showed that the numerical methods properly predict the pressure drop in operating parameters of the heat exchanger, within the uncertainty of experimental data. To optimize the cost and performance, simulation-based duct design technique that offers automated solution was proposed that utilizes most suitable solution for offices (Kabbara *et al.* 2024; Ben-David *et al.* 2019). For human occupancy, thermal environmental conditions include adaptive comfort standard that allows warmer indoor temperatures for naturally ventilated buildings (Ben-David and Waring 2016; de Dear *et al.* 2002). Adaptable building practices with comfort systems in buildings can effectively deal with the demand of changing needs of owners and users and this will help to facilitate a flexible building use (Seuntjens *et al.* 2022). Conventional methods used for the design of the ventilation systems relay on rules of thumb which leads to cost-inefficient and underperforming systems and a simulation-based design driven metaheuristic techniques can optimize the overall system design (Kabbara *et al.* 2017; Ben-

David *et al.* 2019). Pressure drop in the fittings generate substantial quantity and implementing a proper fitting design at an early stage is important to achieve a superior ventilation system (Kabbara *et al.* 2023). Green buildings are healthy, energy efficient, ecofriendly, high ventilation quality and capability of the building to achieve life cycle sustainability is evaluated for the certification (Wei *et al.* 2015). The reviewed literature demonstrates that HVAC duct design in large enclosures has been widely studied using either conventional analytical methods, such as the Equal Friction Method, or numerical techniques including CFD for airflow and thermal comfort evaluation. However, most analytical studies focus primarily on duct sizing and pressure loss calculations without validating airflow uniformity or pressure behavior under realistic operating conditions. Conversely, CFD-based investigations generally analyze airflow distribution and comfort performance in post-designed systems, often without reference to practical, industry-adopted duct sizing methodologies. Furthermore, limited attention has been paid to the influence of duct aspect ratio on pressure variation and airflow uniformity in auditorium-scale HVAC systems. As a result, a clear research gap exists in the integrated assessment of duct aspect ratio–dependent pressure behavior using CFD, combined with analytically designed duct networks based on the Equal Friction Method. The present study addresses this gap by coupling analytical duct sizing with CFD-based numerical analysis to evaluate pressure variations, airflow distribution, and thermal comfort in an auditorium environment, thereby offering a validated and performance-driven HVAC design framework. In the current study, duct design is done using Equal Friction method and its numerical analysis, 3D modeling and CFD simulation is done to study the variation of pressure, temperature and velocity of flow through the main and the sub ducts. Sheet metals made of steel or aluminum with gauge thickness 0.6 mm to 1.6 mm are the most commonly used duct material in HVAC applications. In this duct design, galvanized steel sheets of 16 gauge (1.6 mm thickness) and 18 gauge (1.2 mm thickness) are recommended for main ducts and 20 gauge (1 mm thickness) for sub ducts based on the air flow rate.

## 2. Methodology

### 2.1 Duct layout and Design

A commercial auditorium was selected as the case study, and cooling load calculations were performed to determine the total refrigeration tonnage. Auditorium is of the size of 36m x 22m x 7m (l x b x h) and the total capacity of the auditorium is 850 occupants. Walls are made of laterite stone of 20 cm thickness with cement mix plastering of 1 cm thickness on inside and outside. Ceiling is made of concrete of 17 cm thickness. Total surface area of the 4 walls is 620 sqm, ceiling area is 572 sqm and windows and doors contribute 55 sqm area. Heat gain through 4 walls is calculated and found to be 11.83 kW and heat gain through ceiling is 24.8 kW. Heat gain through windows and doors is 3.24 kW. Infiltration load is 13.2 kW and sensible heat gain from occupants is 59.5kW. Ventilation load is 52.23 kw. Heat gain from electrical equipment and lighting appliances is 3.5 kW. Total sensible heat gain is 168.3 kW. Latent heat gain due to infiltration is 30.5 kW. Latent heat gain from occupants is 42.5 kW. Total latent heat gain is 73 kW. Total heat load is 241 kW or 69 TR. Total number of occupants in the auditorium is 850 and fresh air requirement per person is 0.015 m<sup>3</sup>/s. So total fresh air requirement is 12.75 m<sup>3</sup>/s. Diffusers are selected based on the volume of air it can handle and throw length. A 600mm square diffuser can handle 0.65 m<sup>3</sup>/s of air and hence total number diffusers required is 20. Based on the dimensions of the auditorium, location of the plant room and seating capacity, number and location of diffusers were assigned and layout was made. The plant room is present on the North West corner and two main ducts are considered and they are ABCDEF and GHIJKL, each containing 10 diffusers each. Lengths of main ducts and sub ducts are estimated and the duct layout is given in the **Figure 1**. Based on the number of occupants served by each diffuser, the required airflow rates for the main duct and sub-ducts were calculated. For auditorium applications, an initial air velocity of 8 m/s was selected, as higher velocities tend to increase noise levels, whereas lower velocities may be inadequate to deliver the required airflow to the branch ducts and associated diffusers. Based on the number of occupants served by each diffuser, the airflow rates

through the main duct and sub-ducts were calculated. For auditorium applications, an initial air velocity of 8 m/s was selected, as higher velocities increase noise levels, while lower velocities may be insufficient to deliver the required airflow to the sub-ducts and corresponding diffusers. Since the duct layout is symmetrical, the Equal Friction Method was adopted for the duct design, as it ensures an approximately uniform pressure loss per unit length and thereby promotes balanced airflow across multiple zones. This method simplifies duct sizing and reduces design time while maintaining acceptable airflow velocities and acoustic performance. In addition, it minimizes the requirement for balancing dampers, thereby lowering both installation and operational costs. Using the Equal Friction Method, initial estimates of the equivalent diameter for each duct section, the airflow velocities in the main and branch ducts, and the corresponding mass flow rates were obtained and are presented in **Table 1**.

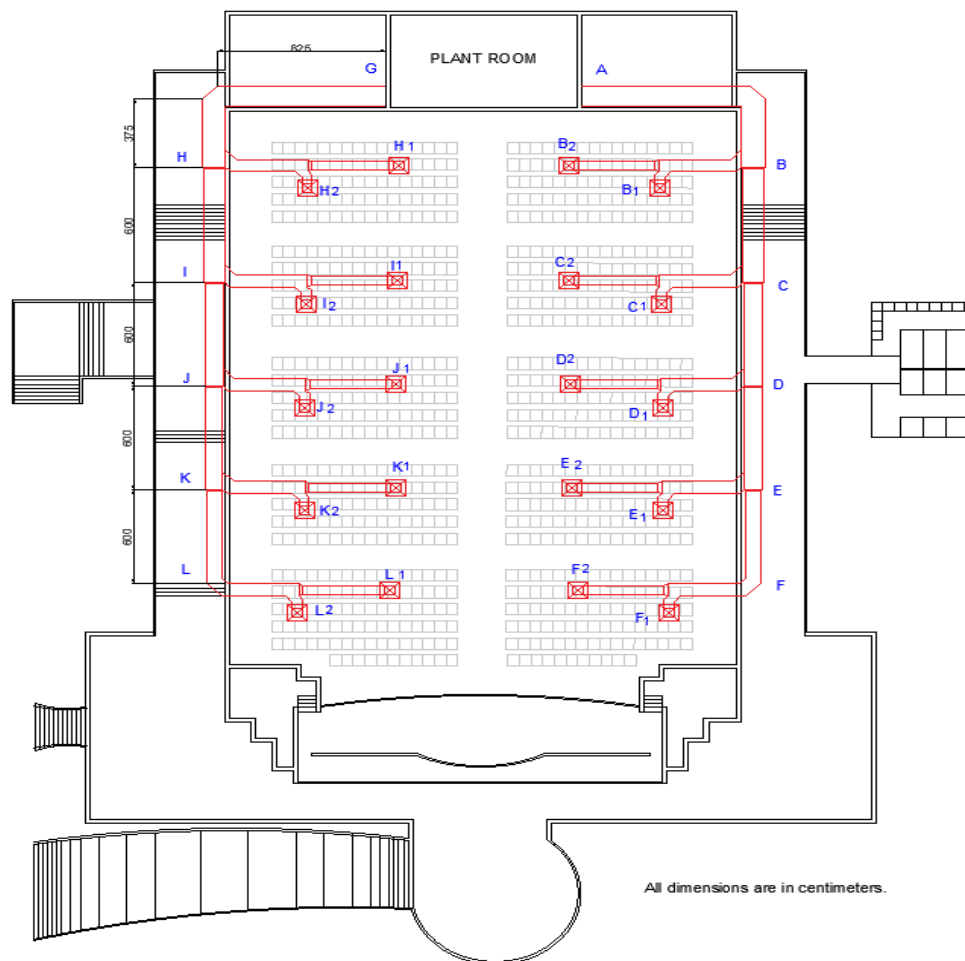


**Figure 1.** Plan of the auditorium and duct layout

**Table 1** Flow rate and equivalent diameter

| Sl no | Section  | Length m | Volume flowrate m <sup>3</sup> /s | Mass flowrate kg/s | Equivalent diameter m | Flow velocity m/s |
|-------|--|----------|-----------------------------------|--------------------|-----------------------|-------------------|
| 1     | GH & AB  | 12       | 6.39                              | 7.97               | 1.0                   | 8                 |
| 2     | HI & BC  | 6        | 5.112                             | 6.376              | 0.9                   | 7.5               |
| 3     | IJ & CD  | 6        | 3.834                             | 4.782              | 0.85                  | 7.2               |
| 4     | JK & DE  | 6        | 2.556                             | 3.188              | 0.77                  | 6.8               |
| 5     | KL & EF  | 6        | 1.278                             | 1.594              | 0.65                  | 6.2               |
| 6     | HH1, BB1, CC1, II1, JJ1, DD1, KK1, EE1, LL1, FF1           | 3.5      | 1.278                             | 1.594              | 0.65                  | 6.2               |
| 7     | H1H2, B1B2, C1C2, I1I2, J1J2, D1D2, K1K2, E1E2, L1L2, F1F2 | 3.5      | 0.639                             | 0.797              | 0.43                  | 4.7               |

## 2.2 Numerical analysis of airflow at different aspect Ratios

Duct friction charts are based on round ducts while in practical applications and corresponding rectangular equivalent ducts are used. Formulas are published by ASHRAE for converting circular equivalent ( $D_e$ ) in to corresponding rectangular duct and these formulas are used to get the dimensions of rectangular ducts for different aspect ratios. For finding out rectangular equivalent of the circular duct, Huebscher equation is used. Different aspect ratios are considered and cross-sectional dimensions of main and sub ducts are calculated for each aspect ratio. Equivalent diameter ( $D_e$ ) is the diameter of a circular duct that has equal pressure loss of a rectangular duct. The Huebscher equation is selected as the basis for converting duct geometries because it is the industry-standard empirical relationship adopted by ASHRAE for maintaining equal friction loss across varying cross-sections. While alternative models like the Tsal formula exist, the Huebscher equation is specifically calibrated for the turbulent flow regimes and standard air densities investigated in this study. Furthermore, it provides higher accuracy for pressure drop prediction than the standard hydraulic diameter, which typically fails to account for the non-uniform shear stress distributions in rectangular corners.

$$D_e = \frac{1.3(ab)^{0.625}}{(a+b)^{0.25}} \quad (1)$$

Using Huebscher equation, corresponding to each equivalent diameter ( $D_e$ ), width (a) and height (b) of the rectangular ducts for the main and sub ducts for different aspect ratios are calculated and are given in **Table 2**. For HVAC ducts of rectangular shape, aspect ratios practically considered are between 1:1 to 1:4. Higher the aspect ratio, higher the pressure loss and noise due to higher turbulence and friction. Lower the aspect ratio, lower the frictional resistance and hence lower the power needed to drive the blower. But lower aspect ratios will compromise ceiling space and hence cause duct installation issues. It may also cause uneven distribution of the conditioned air through different subducts. Un even distribution of conditioned air can be only managed by flow balancing which is done by placing dampers in branch ducts or grills and are manually adjusted to match the design flow rates. But dampers are obstacles which causes dynamic lose and this increases the energy usage. The use of dampers can be avoided if the duct aspect ratio is selected to ensure uniform airflow and minimal deviation from the design conditions. Ducts should be designed and fabricated by considering all the above-mentioned factors. To identify the aspect ratio that results in the minimum variation from the design conditions, multiple aspect ratios were evaluated, and the corresponding CFD models were developed. For sustainable design, the aspect ratios 1:1, 1:1.2, 1:1.4, 1:1.6, 1:1.8, 1:2.0, and 1:2.2 were considered and analyzed.

**Table 2** Duct dimensions corresponding to each equivalent diameter in meter

| De   | 1:1  |      | 1:1.2 |      | 1:1.4 |      | 1:1.6 |      | 1:1.8 |      | 1:2  |      | 1:2.2 |      |
|------|------|------|-------|------|-------|------|-------|------|-------|------|------|------|-------|------|
|      | a    | b    | a     | b    | a     | b    | a     | b    | a     | b    | a    | b    | a     | b    |
| 1.0  | 0.92 | 0.92 | 1.00  | 0.84 | 1.09  | 0.78 | 1.17  | 0.73 | 1.24  | 0.69 | 1.31 | 0.66 | 1.38  | 0.63 |
| 0.9  | 0.82 | 0.82 | 0.90  | 0.75 | 0.98  | 0.70 | 1.09  | 0.66 | 1.12  | 0.62 | 1.18 | 0.59 | 1.24  | 0.57 |
| 0.85 | 0.78 | 0.78 | 0.85  | 0.71 | 0.92  | 0.66 | 0.99  | 0.62 | 1.05  | 0.59 | 1.12 | 0.56 | 1.18  | 0.53 |
| 0.77 | 0.70 | 0.70 | 0.77  | 0.64 | 0.84  | 0.60 | 0.90  | 0.56 | 0.96  | 0.53 | 1.01 | 0.51 | 1.07  | 0.48 |
| 0.65 | 0.60 | 0.59 | 0.65  | 0.54 | 0.71  | 0.50 | 0.76  | 0.47 | 0.81  | 0.45 | 0.85 | 0.43 | 0.90  | 0.41 |
| 0.65 | 0.60 | 0.60 | 0.65  | 0.54 | 0.71  | 0.50 | 0.76  | 0.47 | 0.81  | 0.45 | 0.85 | 0.43 | 0.90  | 0.41 |
| 0.43 | 0.39 | 0.39 | 0.43  | 0.36 | 0.47  | 0.33 | 0.50  | 0.31 | 0.53  | 0.30 | 0.57 | 0.28 | 0.60  | 0.27 |

For the flow through a non-circular duct which involve calculations regarding turbulent flow, hydraulic diameter ( $D_h$ ) is used. Hydraulic diameters ( $D_h$ ) for all equivalent diameters ( $D_e$ ) at different aspect ratios are calculated by using the following equation and are given in the **Table 3**. Here A is the surface area of the channel and P is the wetted perimeter of the duct.

$$D_h = \frac{4A}{P} \quad (2)$$

**Table 3** Hydraulic diameter in meters

| Aspect ratio | 1:1   | 1:1.2 | 1:1.4 | 1:1.6 | 1:1.8 | 1:2   | 1:2.2 |
|--------------|-------|-------|-------|-------|-------|-------|-------|
| De           |       |       |       |       |       |       |       |
| 1.0          | 0.915 | 0.912 | 0.905 | 0.896 | 0.886 | 0.875 | 0.864 |
| 0.90         | 0.823 | 0.820 | 0.815 | 0.806 | 0.797 | 0.788 | 0.778 |
| 0.85         | 0.778 | 0.775 | 0.769 | 0.762 | 0.757 | 0.744 | 0.734 |
| 0.77         | 0.704 | 0.702 | 0.697 | 0.690 | 0.683 | 0.674 | 0.666 |
| 0.65         | 0.595 | 0.592 | 0.588 | 0.583 | 0.576 | 0.569 | 0.562 |
| 0.65         | 0.595 | 0.592 | 0.588 | 0.583 | 0.576 | 0.569 | 0.562 |
| 0.43         | 0.393 | 0.392 | 0.389 | 0.385 | 0.381 | 0.376 | 0.371 |

Galvanized steel sheets are used as the duct material and surface roughness constant ( $\epsilon$ ) for the duct material is taken from properties charts of the material and is 0.0001524 m. Relative roughness ( $k$ ) is calculated by using the following equation and are given in the **Table 4**.

$$k = \frac{\epsilon}{D_h} \quad (3)$$

**Table 4** Relative roughness (k)

| De   | 1:1      | 1:1.2    | 1:1.4    | 1:1.6    | 1:1.8    | 1:2      | 1:2.2    |
|------|----------|----------|----------|----------|----------|----------|----------|
| 1.0  | 0.000166 | 0.000167 | 0.000168 | 0.000170 | 0.000171 | 0.000174 | 0.000176 |
| 0.90 | 0.000185 | 0.000185 | 0.000187 | 0.000189 | 0.000191 | 0.000193 | 0.000196 |
| 0.85 | 0.000196 | 0.000197 | 0.000198 | 0.000199 | 0.000201 | 0.000205 | 0.000207 |
| 0.77 | 0.000216 | 0.000217 | 0.000218 | 0.000221 | 0.000223 | 0.000226 | 0.000232 |
| 0.65 | 0.000256 | 0.000257 | 0.000259 | 0.000262 | 0.000265 | 0.000267 | 0.000272 |
| 0.65 | 0.000256 | 0.000257 | 0.000259 | 0.000262 | 0.000265 | 0.000267 | 0.000272 |
| 0.43 | 0.000388 | 0.000389 | 0.000391 | 0.000396 | 0.000400 | 0.000405 | 0.000410 |

Since hydraulic diameter and velocity are known Reynold's number for each duct section and for each aspect ratio are calculated using the following equation and are tabulated in **Table 5**.

$$k = \frac{VD_h}{\nu} \quad (4)$$

**Table 5** Reynold's number

| De   | 1:1    | 1:1.2  | 1:1.4  | 1:1.6  | 1:1.8  | 1:2    | 1:2.2  |
|------|--------|--------|--------|--------|--------|--------|--------|
| 1.0  | 468630 | 467692 | 464102 | 459487 | 454358 | 448718 | 443077 |
| 0.90 | 395673 | 394231 | 391827 | 387500 | 383173 | 378846 | 374039 |
| 0.85 | 359077 | 357692 | 354923 | 351692 | 349385 | 343385 | 338769 |
| 0.77 | 306872 | 306000 | 303821 | 300769 | 297718 | 293795 | 290308 |
| 0.65 | 236474 | 235282 | 233692 | 231705 | 228923 | 226141 | 223359 |
| 0.65 | 236474 | 235282 | 233692 | 231705 | 228923 | 226141 | 223359 |
| 0.43 | 118040 | 118102 | 116596 | 115994 | 114788 | 113282 | 111776 |

For all the equivalent diameters as the aspect ratio increases, Reynold's number decreases. Using the Reynold's number and relative roughness ( $k$ ), friction factor  $f$  is taken from Moody's chart and is given in **Table 6**.

**Table 6.** Friction factor

| De   | 1:1    | 1:1.2  | 1:1.4  | 1:1.6  | 1:1.8  | 1:2    | 1:2.2  |
|------|--------|--------|--------|--------|--------|--------|--------|
| 1.0  | 0.0155 | 0.0156 | 0.0157 | 0.0158 | 0.0159 | 0.0161 | 0.0163 |
| 0.90 | 0.0160 | 0.0160 | 0.0161 | 0.0162 | 0.0163 | 0.0165 | 0.0167 |
| 0.85 | 0.0165 | 0.0165 | 0.0166 | 0.0166 | 0.0167 | 0.0168 | 0.0172 |
| 0.77 | 0.0168 | 0.0168 | 0.0170 | 0.0171 | 0.0171 | 0.0172 | 0.0176 |
| 0.65 | 0.0170 | 0.0171 | 0.0172 | 0.0174 | 0.0175 | 0.0176 | 0.0180 |
| 0.65 | 0.0170 | 0.0171 | 0.0172 | 0.0174 | 0.0175 | 0.0176 | 0.0180 |
| 0.43 | 0.0195 | 0.0197 | 0.0198 | 0.0199 | 0.0200 | 0.0201 | 0.0204 |

Frictional losses, also referred to as distributed pressure losses, arise from viscous shear between the moving air and the duct wall along the duct length. These losses are governed by duct surface roughness, hydraulic diameter, air velocity, and Reynolds number. They are commonly evaluated using the Darcy–Weisbach equation or the equal-friction method.

$$h_f = \frac{fLV^2}{2gd} \quad (5)$$

As per the definition of the equal friction method, the loss of head per meter length of all the ducts should be same. If the loss of head per meter length of all the ducts are same then the air distribution through the main duct and each of the sub ducts will be uniform and hence will be based on the demand through each diffuser. Head loss due to friction (m of air) per unit length of the duct in main duct and sub ducts for different aspect ratios, their standard deviation (SD) and coefficient of variation (CV) are calculated and are given in the **Table 7**. For each aspect ratio total frictional head loss is also calculated.

**Table 7** Frictional head loss per unit length and total loss. (in m of air).

| De             | 1:1.0    | 1:1.2    | 1:1.4    | 1:1.6    | 1:1.8    | 1:2     | 1:2.2    |
|----------------|----------|----------|----------|----------|----------|---------|----------|
| 1.0            | 0.05526  | 0.05580  | 0.05658  | 0.05752  | 0.05854  | 0.06002 | 0.06154  |
| 0.90           | 0.05573  | 0.05594  | 0.05663  | 0.05762  | 0.05863  | 0.06003 | 0.06154  |
| 0.85           | 0.05604  | 0.05625  | 0.05669  | 0.05756  | 0.05829  | 0.05966 | 0.06192  |
| 0.77           | 0.05624  | 0.05640  | 0.05748  | 0.05841  | 0.05900  | 0.06014 | 0.06228  |
| 0.65           | 0.05600  | 0.05659  | 0.05731  | 0.05847  | 0.05953  | 0.06060 | 0.06275  |
| 0.65           | 0.05600  | 0.05659  | 0.05731  | 0.05847  | 0.05953  | 0.06060 | 0.06275  |
| 0.43           | 0.05587  | 0.05658  | 0.05731  | 0.05819  | 0.05910  | 0.06019 | 0.06191  |
| Average        | 0.05588  | 0.05631  | 0.05704  | 0.05803  | 0.05895  | 0.06018 | 0.06210  |
| SD             | 0.000291 | 0.000302 | 0.000361 | 0.000415 | 0.000448 | 0.00031 | 0.000474 |
| CV             | 0.56     | 0.536    | 0.633    | 0.715    | 0.759    | 0.515   | 0.763    |
| Friction loss. | 3.965    | 4.001    | 4.054    | 4.124    | 4.191    | 4.277   | 4.411    |

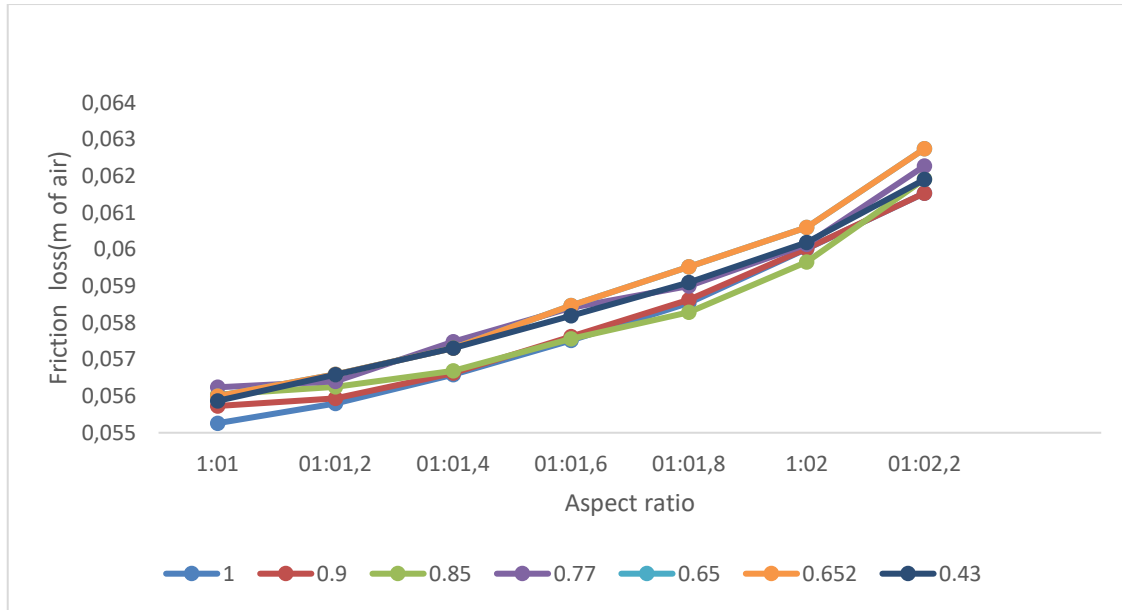


**Figure 2.** Friction loss variation for different equivalent diameters.

Statistical analysis shows that the standard deviation of the frictional loss for the various aspect ratios lies in the range of 0.000291 to 0.000474, indicating a very small spread in the data. This confirms that, for a given aspect ratio, the frictional losses across the different duct sections are closely clustered and exhibit negligible deviation from the mean value. This trend is consistently observed for all aspect ratios considered. Furthermore, the coefficient of variation (CV) is less than 10%, demonstrating strong agreement among the data sets. These results analytically confirm that when ducts are designed using the Equal Friction Method, the frictional loss per unit length remains approximately constant throughout the duct network, thereby ensuring uniform air distribution, provided that the ducts are fabricated in accordance with the design specifications. As illustrated in Fig. 6, the frictional head loss per unit length remains nearly constant for each aspect ratio. However, the magnitude of the frictional loss increases with increasing aspect ratio (**Figure 2**). The minimum average frictional head loss occurs for an aspect ratio of 1:1, with a value of 0.05588 m of air per metre of duct length (approximately 0.7 Pa/m). As the aspect ratio increases, the frictional loss also increases, reaching a maximum of 0.0621 m of air per metre of duct length (approximately 0.8 Pa/m) for an aspect ratio of 1:2.2. The computed friction losses are in good agreement with recommended

design values. The low standard deviations further confirm that variations from the corresponding mean values are minimal, indicating strong consistency and reliability of the results.

### 2.3 Computational Analysis of the air flow through the duct.

The total mass flow rate of air supplied from the plant room into the main duct is 7.97 kg/s. Conditioned air at a temperature of 10 °C enters the main duct from the plant room and, as it flows through the duct system, a portion of the air is diverted into the sub-ducts and subsequently delivered to the diffusers, from where it is supplied to the conditioned space. The remaining air continues to flow through the main duct. The primary objective is to distribute the air uniformly among all ten diffusers with minimum pressure loss, such that the mass flow rate through each diffuser is 0.797 kg/s. The simulation parameters and boundary conditions are described in the following paragraph. The flow simulations were performed using Flow Wizard software. Three-dimensional duct models corresponding to the design values for all seven aspect ratios were created using SOLIDWORKS. The simulation parameters and boundary conditions were assigned based on the specified flow conditions. One of the generated CFD models is shown in **Figure 3**.

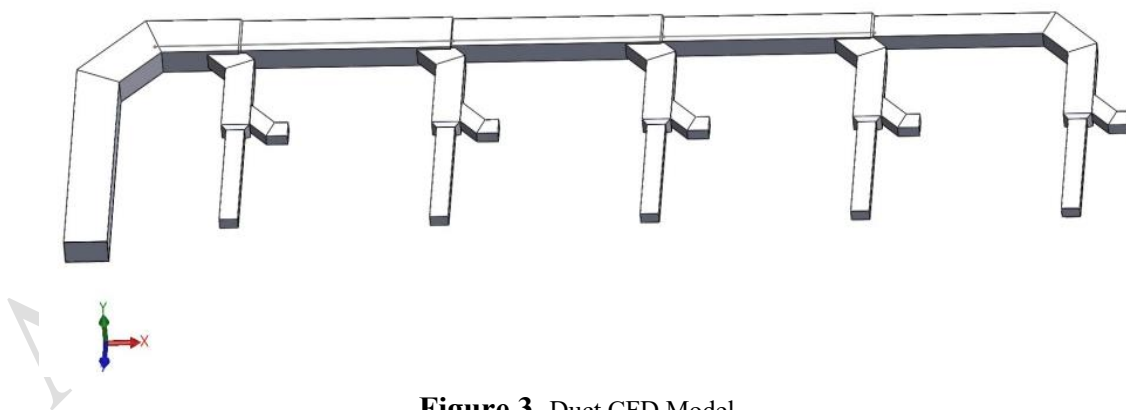


**Figure 3.** Duct CFD Model.

The simulations were carried out using the Flow Wizard CFD solver for steady-state internal airflow. A mass flow inlet boundary condition of 7.97 kg/s at a temperature of 10 °C and relative humidity of 50% was imposed at the main duct inlet. Each diffuser outlet was modelled as a pressure outlet with atmospheric static pressure (1.01325 bar). The duct walls were treated as no-slip and

adiabatic. Gravity was included in the negative y-direction with a magnitude of 9.81 m/s<sup>2</sup>. The operating pressure and ambient conditions were set to 1.01325 bar, 35 °C, and 50% relative humidity. The objective of the simulation was to achieve a uniform distribution of mass flow through all ten diffusers, with a target flow rate of 0.797 kg/s per diffuser. Simulations were performed for all seven aspect ratios, and the corresponding results were obtained. The mass flow rates from each of the ten diffusers, expressed in kg/s, are presented in **Table 8**. The table also reports the mean value, absolute deviation, standard deviation (SD), and coefficient of variation (CV) for each case.

**Table 8** Mass flow rates in different diffusers obtained from CFD simulations and their statistical analysis.

| Diffusers          | 1:1.0    | 1:1.2    | 1:1.4    | 1:1.6    | 1:1.8    | 1:2.0    | 1:2.2    |
|--------------------|----------|----------|----------|----------|----------|----------|----------|
| 1                  | -0.64695 | -0.50434 | -0.54788 | -0.62213 | -0.58041 | -0.50502 | -0.61627 |
| 2                  | -0.63051 | -0.62320 | -0.67409 | -0.67041 | -0.51374 | -0.58440 | -0.63047 |
| 3                  | -0.81455 | -0.69699 | -0.75916 | -0.79642 | -0.76012 | -0.69681 | -0.67367 |
| 4                  | -0.75615 | -0.78301 | -0.82282 | -0.84947 | -0.85238 | -0.78248 | -0.73315 |
| 5                  | -0.89245 | -0.80078 | -0.82435 | -0.79290 | -0.79616 | -0.80213 | -0.80509 |
| 6                  | -0.82164 | -0.85123 | -0.84397 | -0.83689 | -0.85051 | -0.84953 | -0.89492 |
| 7                  | -0.98414 | -0.92533 | -0.90217 | -0.86702 | -0.93824 | -0.92601 | -0.90044 |
| 8                  | -0.65545 | -0.93880 | -0.90066 | -0.86159 | -0.92759 | -0.97990 | -0.93107 |
| 9                  | -0.92503 | -0.94676 | -0.84592 | -0.84509 | -0.89695 | -0.94471 | -0.90525 |
| 10                 | -0.82236 | -0.89952 | -0.84900 | -0.83805 | -0.86392 | -0.89899 | -0.87968 |
| Average            | -0.797   | -0.797   | -0.797   | -0.797   | -0.797   | -0.797   | -0.797   |
| Absolute deviation | 0.189    | 0.29266  | 0.24912  | 0.17587  | 0.28426  | 0.2919   | 0.1807   |
| SD                 | 0.132    | 0.1485   | 0.110    | 0.08001  | 0.1437   | 0.158    | 0.130    |
| CV                 | 16.6     | 18.6     | 13.8     | 10.0     | 18.0     | 19.8     | 16.3     |

For an aspect ratio of 1:1, the mass flow rates supplied to the four diffusers are below the design values; consequently, three dampers are required to obtain a uniform flow distribution, with two installed in the main duct and one in the sub-duct. The corresponding simulation convergence behaviour is presented in **Figure 4a**. Increasing the aspect ratio to 1:1.2 still results in sub-design mass flow rates at the four diffusers; however, uniformity can be achieved using only two dampers, both of which are installed in the main duct. The associated simulation convergence curves are shown in **Figure 4b**.

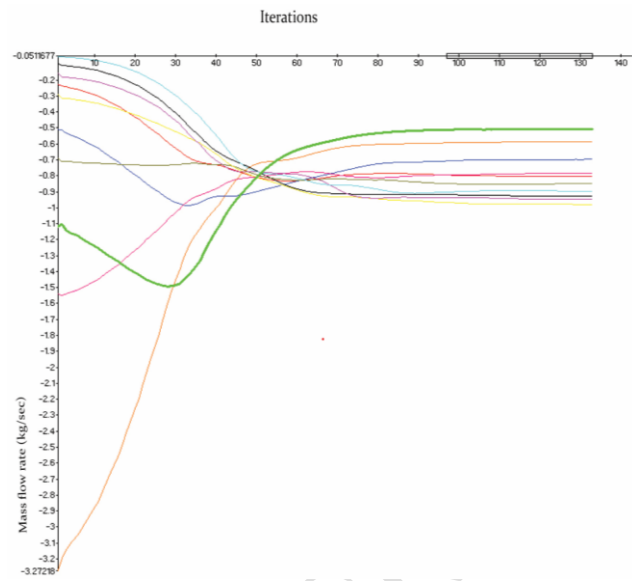
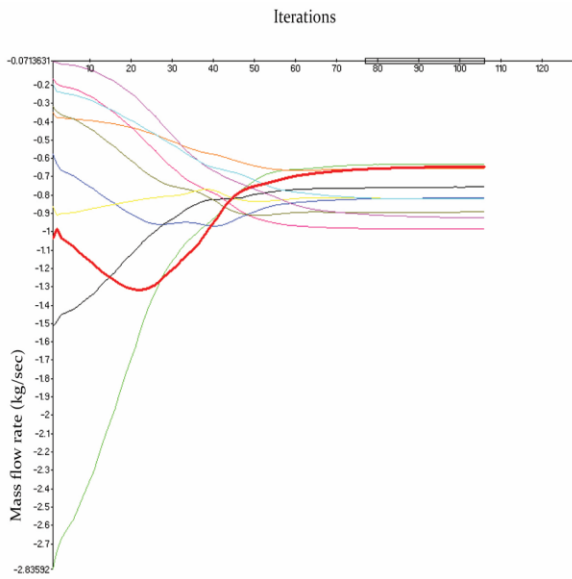


**Figure 4a** Mass flow rates vs Iteration (Aspect Ratio 1:1.0) **Figure 8b** Mass flow rates vs Iteration (Aspect Ratio 1:1.2)

At an aspect ratio of 1:1.4, the mass flow rates delivered to the three diffusers also remain below the design condition, and two dampers are again required, with one installed in the main duct and the other in the sub-duct to ensure uniform distribution. The corresponding simulation convergence curves are illustrated in **Figure 4c**. At an aspect ratio of 1:1.6, the mass flow rates delivered to the two diffusers remain below the design condition, and to remaining diffusers are as per design. In this case one damper is required, which is installed in the main duct to ensure uniform distribution. The corresponding simulation convergence curves are illustrated in **Figure 4d**.

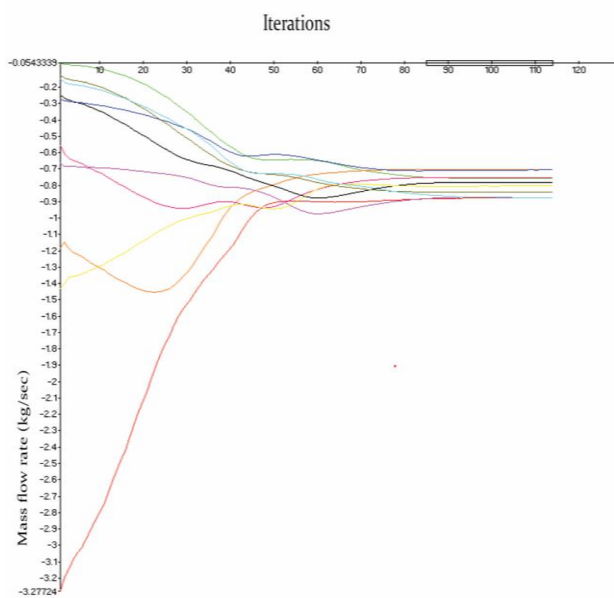
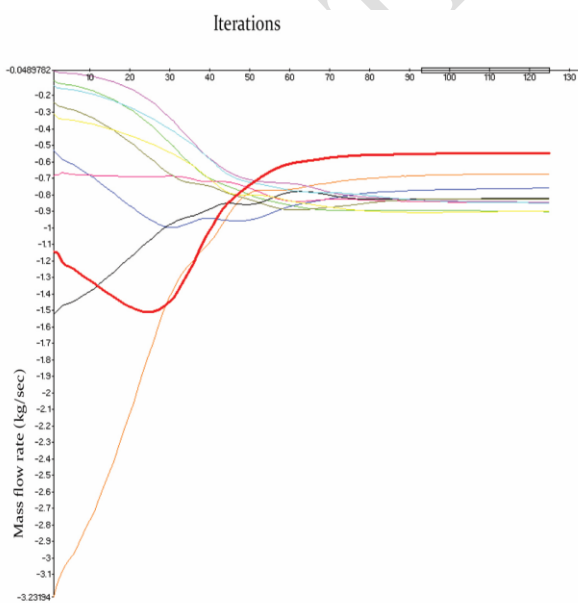


**Figure 4c** Mass flow rates vs Iteration (Aspect Ratio 1:1.4) **Fig. 4d** Mass flow rates vs Iteration (Aspect Ratio 1:1.6)

Further increasing the aspect ratio to 1:1.8 required the installation of two dampers, one in the main

duct and the other in the sub-duct. The corresponding simulation convergence curves are presented in **Figure 4e**. For higher aspect ratios of 1:2.0 and 1:2.2, two dampers were also required in each case; however, both were installed in the main duct. The corresponding simulation convergence curves for these cases are shown in **Figure 4f** and **Figure 4g**, respectively.

Statistical analysis of the mass flow rates at different aspect ratios indicates that the minimum deviation from the design condition occurs at an aspect ratio of 1:1.6. The simulation results for different aspect ratios (1:1.0 to 1:2.2) reveal varying levels of uniformity in the distribution of conditioned air across the ten diffusers. The highest level of convergence in the simulation curves is also observed at the aspect ratio 1:1.6.

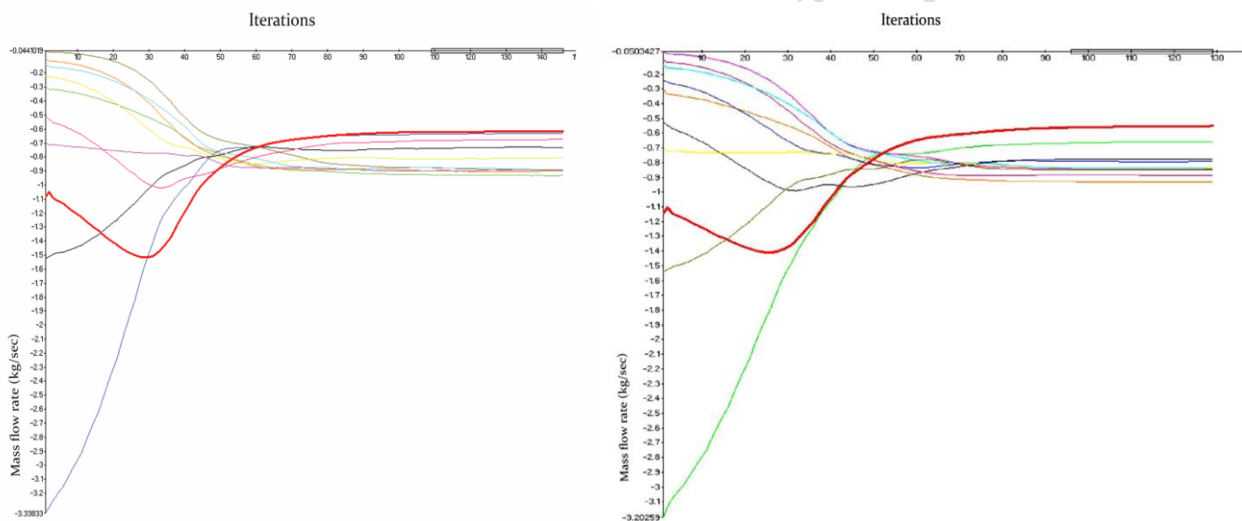


**Figure 4e** Mass flow rates vs Iteration (Aspect Ratio 1:1.8) **Figure 4f** Mass flow rates vs Iteration (Aspect Ratio 1:2.0)

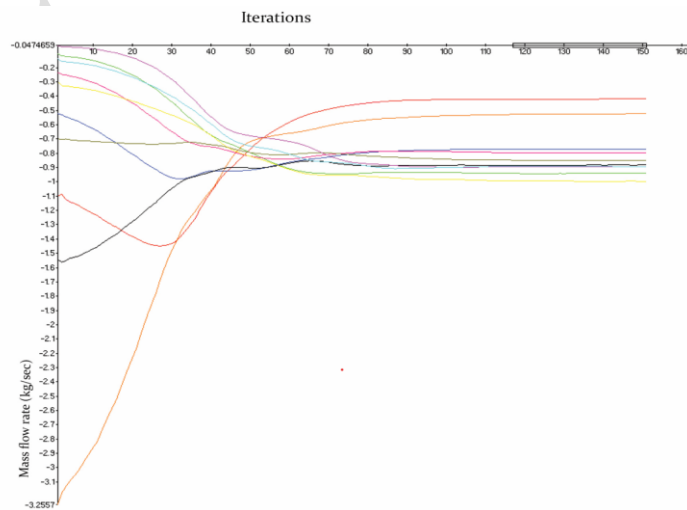


**Figure 4g** Mass flow rates vs Iteration (Aspect Ratio 1:2.2).

Static pressure in an HVAC system is generated by the fan, which adds energy to the air and raises its total and static pressure. Air enters side or sub-ducts due to the static pressure difference between the main duct and the branch. When the velocity in the main duct is high, a larger fraction of the total pressure is converted into velocity pressure, reducing the static pressure available at the branch junction. As a result, less air enters the sub-ducts due to the high main duct velocity. Therefore, the initial diffusers (1 and 2) do not receive adequate airflow. As air is progressively extracted by upstream branches, the airflow rate and velocity in the main duct decrease along its length. This reduction in velocity leads to a corresponding increase in static pressure downstream. As the velocity in the main duct decreases downstream, a sufficient quantity of air enters the remaining sub-ducts, and consequently the flow rates through the remaining diffusers meet the requirement.

As illustrated in **Figure 5a**, the temperature distribution shows minimal variation at the diffuser exits, suggesting that thermal uniformity is achieved across all outlets. **Figure 5b** presents the pressure distribution, which remains uniform across the entire duct network. This indicates balanced pressure losses, contributing to equalized flow delivery. Furthermore, the velocity distribution shown in **Figure 5c** reveals that airflow velocities in both the main and sub-ducts closely match the design targets. Specifically, the exit velocities range from **4.1 m/s to 5.3 m/s**, aligning well with the **design velocity of 4.7 m/s**. This confirms that the system delivers the intended airflow rate to each diffuser. These findings validate the effectiveness of the duct design and demonstrate that the aspect ratio of 1:1.6 provides optimal conditions for uniform air distribution, minimal thermal deviation, and balanced pressure and velocity profiles.

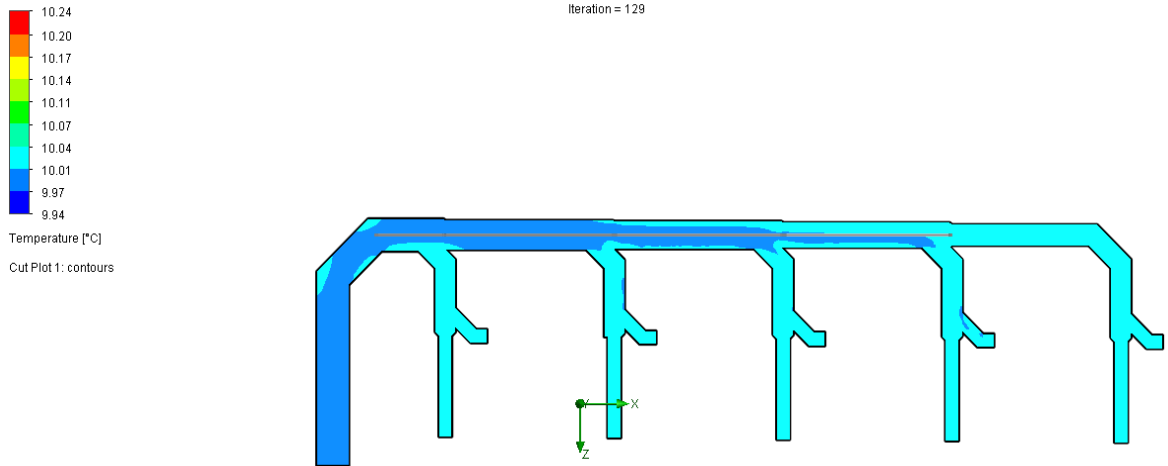


**Figure 5a** Cut plot contour of Temperature distribution for the aspect ratio 1:1.6.

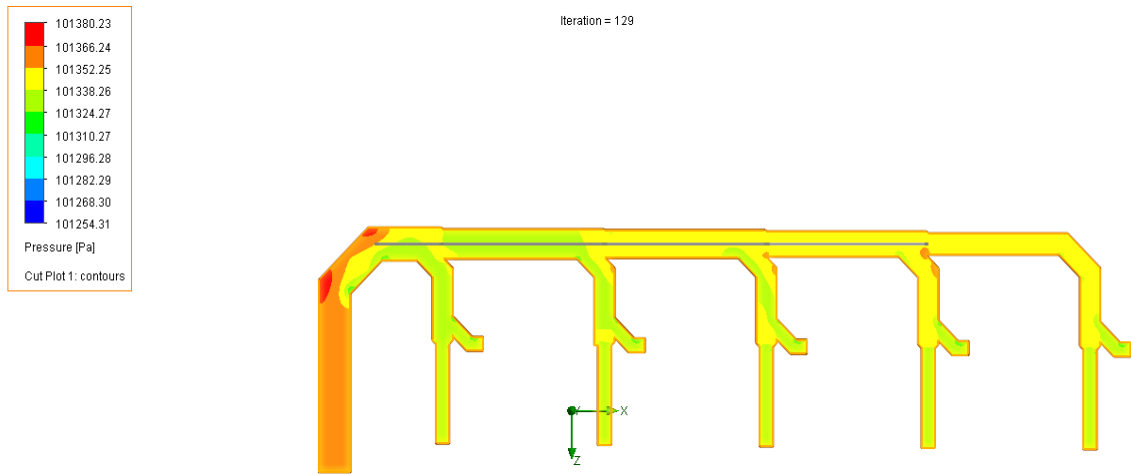


**Figure 5b** Cut plot contour of Pressure distribution for the aspect ratio 1:1.6.

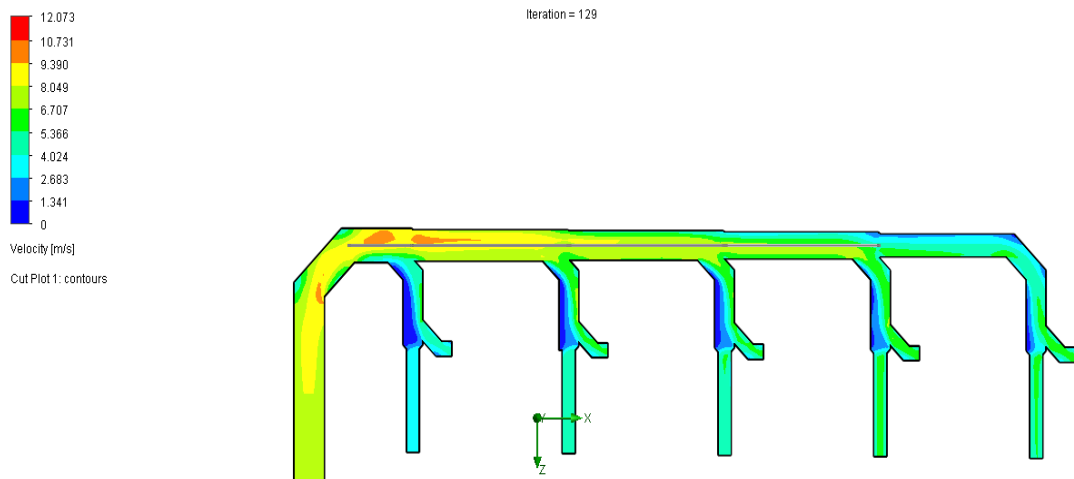


**Figure 5c** Cut plot contour of Velocity distribution for the aspect ratio 1:1.6.

### 3. Calculation of total loses in the ducts.

Friction loss or major loss is the pressure loss due friction between the moving air and the inner surface of the duct. This is already calculated and are tabulated in Table 7. Local losses, also

referred to as minor or dynamic losses, arise from flow disturbances caused by geometric discontinuities and fittings in the duct system, such as bends, tees, transitions, dampers, and diffusers. These elements induce flow separation, secondary flows, and turbulence, resulting in additional pressure losses beyond the distributed frictional losses. Local losses are commonly quantified using dimensionless loss coefficient ( $C_o$  -values) that relate the pressure drop to the dynamic pressure of the flow. Although termed “minor,” their cumulative effect can be significant in complex duct networks and must be accounted for in accurate system design and fan selection. The following Minor Loss equation is used to determine dynamic losses in different fittings and that due to geometry changes.

$$H_l = \frac{C_o \rho V^2}{2} \quad (6)$$

Here,  $C_o$  is a constant whose values are obtained from standard tables. Depending on the type of fitting, the values of  $C_o$  for dampers, elbows, and contractions are taken from ASHRAE HANDBOOK 2001 and are shown as **Table 9a**, **Table 9b**, and **Table 9c**, respectively.

**Table 9a** Damper dimensionless coefficient  $C_o$

**CR9-1 Damper, Butterfly**

| $H/W$ | $C_o$ Values |      |      |      |       |       |       |        |        |       |
|-------|--------------|------|------|------|-------|-------|-------|--------|--------|-------|
|       | $\theta$     |      |      |      |       |       |       |        |        |       |
|       | 0            | 10   | 20   | 30   | 40    | 50    | 60    | 65     | 70     | 90    |
| 0.12  | 0.04         | 0.30 | 1.10 | 3.00 | 8.00  | 23.00 | 60.00 | 100.00 | 190.00 | 99999 |
| 0.25  | 0.08         | 0.33 | 1.18 | 3.30 | 9.00  | 26.00 | 70.00 | 128.00 | 210.00 | 99999 |
| 1.00  | 0.08         | 0.33 | 1.18 | 3.30 | 9.00  | 26.00 | 70.00 | 128.00 | 210.00 | 99999 |
| 2.00  | 0.13         | 0.35 | 1.25 | 3.60 | 10.00 | 29.00 | 80.00 | 155.00 | 230.00 | 99999 |

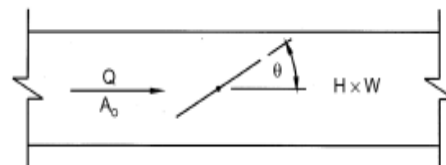


**Table 9b** Elbow dimensionless coefficient  $C_o$

**CR3-6 Elbow, Mitered**

| $\theta$ | $C_o$ Values |      |      |      |      |      |      |      |      |      |      |
|----------|--------------|------|------|------|------|------|------|------|------|------|------|
|          | $H/W$        |      |      |      |      |      |      |      |      |      |      |
|          | 0.25         | 0.50 | 0.75 | 1.00 | 1.50 | 2.00 | 3.00 | 4.00 | 5.00 | 6.00 | 8.00 |
| 20       | 0.08         | 0.08 | 0.08 | 0.07 | 0.07 | 0.07 | 0.06 | 0.06 | 0.05 | 0.05 | 0.05 |
| 30       | 0.18         | 0.17 | 0.17 | 0.16 | 0.15 | 0.15 | 0.13 | 0.13 | 0.12 | 0.12 | 0.11 |
| 45       | 0.38         | 0.37 | 0.36 | 0.34 | 0.33 | 0.31 | 0.28 | 0.27 | 0.26 | 0.25 | 0.24 |
| 60       | 0.60         | 0.59 | 0.57 | 0.55 | 0.52 | 0.49 | 0.46 | 0.43 | 0.41 | 0.39 | 0.38 |
| 75       | 0.89         | 0.87 | 0.84 | 0.81 | 0.77 | 0.73 | 0.67 | 0.63 | 0.61 | 0.58 | 0.57 |
| 90       | 1.30         | 1.27 | 1.23 | 1.18 | 1.13 | 1.07 | 0.98 | 0.92 | 0.89 | 0.85 | 0.83 |

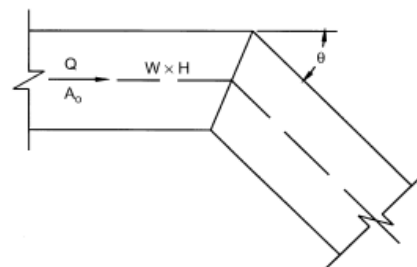


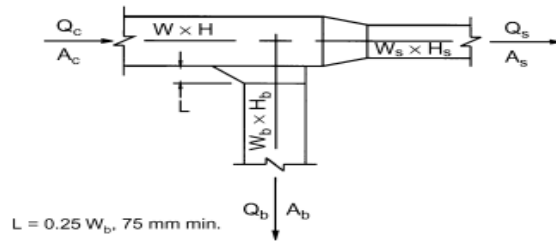
**Table 9c** Diverging dimensionless coefficient  $C_o$

**SR5-13 Tee, 45 Degree Entry Branch, Diverging**

|           |       | $C_b$ Values |      |      |      |      |      |      |      |     |
|-----------|-------|--------------|------|------|------|------|------|------|------|-----|
|           |       | $Q_b/Q_c$    |      |      |      |      |      |      |      |     |
| $A_b/A_c$ |       | 0.1          | 0.2  | 0.3  | 0.4  | 0.5  | 0.6  | 0.7  | 0.8  | 0.9 |
| 0.1       | 0.73  | 0.34         | 0.32 | 0.34 | 0.35 | 0.37 | 0.38 | 0.39 | 0.40 |     |
| 0.2       | 3.10  | 0.73         | 0.41 | 0.34 | 0.32 | 0.32 | 0.33 | 0.34 | 0.35 |     |
| 0.3       | 7.59  | 1.65         | 0.73 | 0.47 | 0.37 | 0.34 | 0.32 | 0.32 | 0.32 |     |
| 0.4       | 14.20 | 3.10         | 1.28 | 0.73 | 0.51 | 0.41 | 0.36 | 0.34 | 0.32 |     |
| 0.5       | 22.92 | 5.08         | 2.07 | 1.12 | 0.73 | 0.54 | 0.44 | 0.38 | 0.35 |     |
| 0.6       | 33.76 | 7.59         | 3.10 | 1.65 | 1.03 | 0.73 | 0.56 | 0.47 | 0.41 |     |
| 0.7       | 46.71 | 10.63        | 4.36 | 2.31 | 1.42 | 0.98 | 0.73 | 0.58 | 0.49 |     |
| 0.8       | 61.79 | 14.20        | 5.86 | 3.10 | 1.90 | 1.28 | 0.94 | 0.73 | 0.60 |     |
| 0.9       | 78.98 | 18.29        | 7.59 | 4.02 | 2.46 | 1.65 | 1.19 | 0.91 | 0.73 |     |

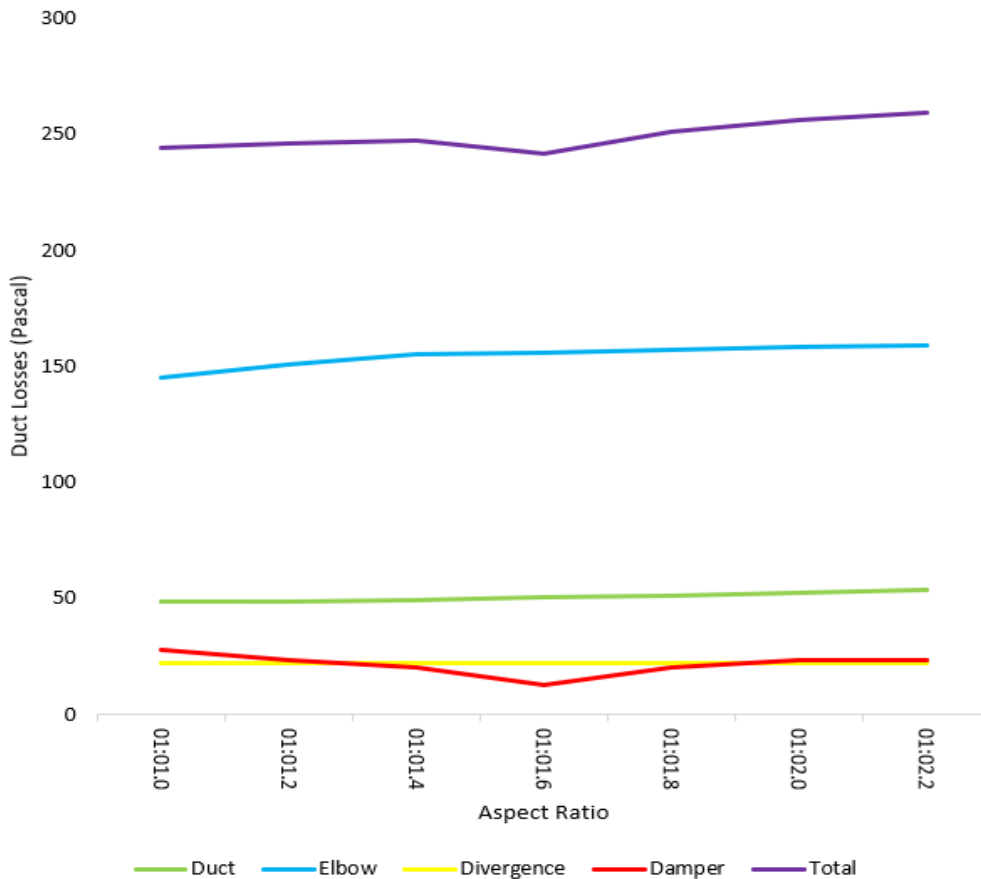
  

|           |       | $C_x$ Values |      |      |      |      |      |      |      |     |
|-----------|-------|--------------|------|------|------|------|------|------|------|-----|
|           |       | $Q_s/Q_c$    |      |      |      |      |      |      |      |     |
| $A_s/A_c$ |       | 0.1          | 0.2  | 0.3  | 0.4  | 0.5  | 0.6  | 0.7  | 0.8  | 0.9 |
| 0.1       | 0.04  |              |      |      |      |      |      |      |      |     |
| 0.2       | 0.98  | 0.04         |      |      |      |      |      |      |      |     |
| 0.3       | 3.48  | 0.31         | 0.04 |      |      |      |      |      |      |     |
| 0.4       | 7.55  | 0.98         | 0.18 | 0.04 |      |      |      |      |      |     |
| 0.5       | 13.18 | 2.03         | 0.49 | 0.13 | 0.04 |      |      |      |      |     |
| 0.6       | 20.38 | 3.48         | 0.98 | 0.31 | 0.10 | 0.04 |      |      |      |     |
| 0.7       | 29.15 | 5.32         | 1.64 | 0.60 | 0.23 | 0.09 | 0.04 |      |      |     |
| 0.8       | 39.48 | 7.55         | 2.47 | 0.98 | 0.42 | 0.18 | 0.08 | 0.04 |      |     |
| 0.9       | 51.37 | 10.17        | 3.48 | 1.46 | 0.67 | 0.31 | 0.15 | 0.07 | 0.04 |     |



**Table 10** Total duct loss in Pascals

|            | 1:1.0  | 1:1.2  | 1:1.4  | 1:1.6  | 1:1.8  | 1:2.0  | 1:2.2  |
|------------|--------|--------|--------|--------|--------|--------|--------|
| Duct       | 48.62  | 49.06  | 49.71  | 50.57  | 51.39  | 52.45  | 54.09  |
| Elbow      | 145.6  | 151.16 | 155.5  | 156.3  | 157.59 | 158.44 | 159.3  |
| Divergence | 22.12  | 22.12  | 22.12  | 22.12  | 22.12  | 22.12  | 22.12  |
| Damper     | 27.89  | 23.81  | 20.28  | 12.67  | 20.28  | 23.81  | 23.81  |
| Total      | 244.26 | 246.17 | 247.61 | 241.66 | 251.38 | 256.53 | 259.32 |



**Figure 6** Duct Losses vs Aspect Ratio

#### **4. Result and discussions**

The cooling load of the auditorium was calculated, and the total cooling requirement was determined. Based on the seating arrangement, a duct layout sketch was prepared and the duct system was designed using the Equal Friction Method. The circular duct dimensions were then converted into equivalent rectangular ducts for seven different aspect ratios, and numerical calculations were performed for each case to determine the friction losses in the ducts. A statistical analysis of these results was subsequently carried out. The analysis shows that, for a given aspect ratio, the friction loss per unit length remains the same for all ducts. It is also observed that the friction loss per unit length increases with increasing aspect ratio.

For the computational analysis of airflow through the duct system, CFD models were developed for all the considered aspect ratios and simulations were performed. The CFD results include the mass flow rates at the individual diffusers, mass flow rate convergence histories with respect to iteration number, and contour plots of velocity, temperature, and pressure distributions within the duct.

A statistical analysis of the CFD results was then carried out to identify the aspect ratio that produces the minimum deviation of mass flow rate from the design condition. The analysis indicates that, as the aspect ratio increases from 1:1, the deviation of mass flow rate from the design value decreases. This trend continues up to an aspect ratio of 1:1.6. Beyond this value, further increases in aspect ratio result in a divergence of the mass flow rates from the design condition. Since the SD, CV, and absolute variation are minimum for this aspect ratio, it exhibits the least deviation from the design condition.

For an aspect ratio of 1:1, the mass flow rates supplied to four diffusers are lower than the design values. Consequently, three dampers are required to achieve uniform flow distribution, with

two installed in the main duct and one in the sub-duct. When the aspect ratio is increased to 1:1.2, the mass flow rates at the four diffusers remain below the design condition; however, uniform distribution can be achieved using only two dampers, both installed in the main duct. At an aspect ratio of 1:1.4, the mass flow rates delivered to three of the diffusers are still lower than the design values, and two dampers are again required, with one installed in the main duct and the other in the sub-duct to ensure uniformity. For an aspect ratio of 1:1.6, the mass flow rates delivered to two of the diffusers remain below the design condition, while the remaining diffusers operate at the design values. In this case, only one damper is required, which is installed in the main duct to obtain a uniform flow distribution. Further increasing the aspect ratio to 1:1.8 necessitates the installation of two dampers, one in the main duct and one in the sub-duct. For higher aspect ratios of 1:2.0 and 1:2.2, two dampers are also required in each case; however, both are installed in the main duct.

The influence of duct aspect ratio on pressure losses was examined by analyzing both frictional losses and minor losses arising from elbows, dampers, and duct contractions. The relationship between duct friction loss and aspect ratio is presented in **Table 10**, and the corresponding trend is illustrated in **Figure 6**. The **duct friction loss** is minimum at an aspect ratio of **1:1 (48.62 Pa)** and increases gradually with increasing aspect ratio, reaching a maximum of **54.09 Pa** at **1:2.2**. This trend is consistent with increased wetted perimeter and hydraulic diameter reduction, as described in ASHRAE duct design guidelines.

**Elbow losses**, which constitute the dominant portion of the minor losses, also increase with aspect ratio. The minimum elbow pressure loss of **145.6 Pa** occurs at an aspect ratio of **1:1**, while the maximum loss is observed at **1:2.2**. In contrast, **divergence losses remain constant**, indicating negligible dependence on duct geometry within the investigated range.

The **damper pressure loss** exhibits a non-linear relationship with aspect ratio, primarily governed by the number of dampers required and their placement within the duct system. The maximum

damper loss of **27.89 Pa** occurs at an aspect ratio of **1:1**, where three dampers are required, two installed in the high-velocity main duct and one in the lower velocity sub duct. For an aspect ratio of **1:1.2**, two dampers were required, both installed in the main duct, resulting in a total pressure loss of **23.81 Pa**. When the aspect ratio was increased to **1:1.4**, two dampers were still necessary; however, one was installed in the main duct and the other in the sub-duct, which reduced the pressure loss to **20.28 Pa**. For an aspect ratio of **1:1.6**, only a single damper was required, placed in the main duct. Consequently, the pressure loss was minimized and was calculated to be **12.67 Pa**, which is the lowest among all the cases studied. Further increasing the aspect ratio to **1:1.8** again necessitated two dampers, one in the main duct and one in the sub-duct, leading to an increase in pressure loss to **20.28 Pa**. For higher aspect ratios of **1:2.0** and **1:2.2**, two dampers were required in each case, both located in the main duct, and the corresponding pressure loss increased further to **23.81 Pa**. These results clearly indicate that the **minimum damper-induced pressure loss occurs at an aspect ratio of 1:1.6**, making it the most hydraulically efficient configuration among those investigated.

For typical HVAC design practice, the **pressure loss across a diffuser** (also called diffuser pressure drop or terminal loss) generally lies in the range 8 to 15 Pascals. Taking an average of 12 Pascals (irrespective of the aspect ratio), total terminal loss will be 120 Pascals as there are 10 diffusers. The total pressure loss in the duct system (including diffuser losses) is maximum for the aspect ratio 1:2.2, with a value of 379.32 Pa, and minimum for the aspect ratio 1:1.6, with a value of 361.66 Pa, representing a reduction of 4.65%. These results indicate that an aspect ratio of 1:1.6 provides an optimal balance by minimizing duct energy losses while maintaining acceptable frictional and minor losses. This finding has practical significance for HVAC duct design, as minimizing pressure losses directly reduces fan power requirements and improves overall system energy efficiency.

## 5. Conclusions

This study systematically investigated the influence of duct aspect ratio on airflow distribution, pressure losses, and hydraulic performance in an auditorium HVAC duct system using numerical calculations, CFD simulations, and statistical analysis. Circular ducts designed using the Equal Friction Method were converted into equivalent rectangular ducts with aspect ratios ranging from 1:1 to 1:2.2, and their performance was evaluated in terms of friction losses, flow uniformity, damper requirements, and total pressure losses. The results show that increasing the aspect ratio leads to higher friction losses per unit length due to increased wetted perimeter and reduced hydraulic diameter. CFD analysis further revealed that deviation of mass flow rate from the design condition decreases as the aspect ratio increases from 1:1 to 1:1.6, beyond which further increases cause a deterioration in flow uniformity. Correspondingly, the number and placement of dampers required to achieve uniform distribution varied with aspect ratio and strongly influenced damper-induced pressure losses. Among all cases studied, an aspect ratio of 1:1.6 was identified as the optimal configuration. This ratio required only one damper, exhibited the lowest damper pressure loss (12.67 Pa), and resulted in the minimum total system pressure loss of 361.66 Pa, which is 4.65% lower than the maximum observed value at an aspect ratio of 1:2.2. Although friction and elbow losses increased monotonically with aspect ratio, the reduction in damper losses at 1:1.6 more than compensated for this increase, leading to the most hydraulically efficient overall performance. Therefore, the study concludes that a rectangular duct aspect ratio of 1:1.6 provides the best compromise between flow uniformity, controllability, and energy efficiency for the investigated duct configuration. This finding has direct practical relevance for HVAC system design, as selecting an appropriate aspect ratio can significantly reduce pressure losses, minimize fan power consumption, and improve overall system performance without additional control devices or complexity.

## References

- Aravinda D., Karthik T., Kunabeva N.D. (2017), Numerical analysis of airflow characteristics in heating, ventilating and air conditioning (HVAC) duct, *International Journal of Innovative Research in Science, Engineering and Technology*, 6(12), 22653–22668.
- Bamodu O., Xia L., Tang L. (2017), A numerical simulation of air distribution in an office room ventilated by 4-way cassette air-conditioner, *Energy Procedia*, 105, 2506–2511.
- Ben-David T., Rackes A., Lo L.J., Wen J., Waring M.S. (2019), Optimizing ventilation: theoretical study on increasing rates in offices to maximize occupant productivity with constrained additional energy use, *Building and Environment*, 166, 106314.
- Ben-David T., Waring M.S. (2016), Impact of natural versus mechanical ventilation on simulated indoor air quality and energy consumption in offices in fourteen U.S. cities, *Building and Environment*, 104, 320–336.
- Chowdhury A.A., Rasul M.G., Khan M.M.K. (2022), Thermal performance assessment of retrofitted building using an integrated energy and computational fluid dynamics (IE-CFD) approach, *Energy Reports*, 8, 709–719.
- de Dear R.J., Brager G.S. (2002), Thermal comfort in naturally ventilated buildings: revisions to ASHRAE Standard 55, *Energy and Buildings*, 34(6), 549–561.
- Gao R., Wang M., Guo W. (2021), Study of the shape optimization of a variable diameter in a ventilation and air-conditioning duct based on Boltzmann function, *Journal of Building Engineering*, 43, 102833.
- Kabbara Z., Jorens S., Ahmadian E., Verhaert I. (2023), Improving HVAC ductwork designs while considering fittings at an early stage, *Building and Environment*, 237, 110272.
- Kabbara Z., Jorens S., Matbouli H., Van Thillo J., Verhaert I. (2023), Heuristic optimization for designing centralized air distribution systems in non-residential buildings, *Energy and Buildings*,

292, 113161.

Kabbara Z., Jorens S., Seuntjens O., Verhaert I. (2024), Simulation-based optimization method for retrofitting HVAC ductwork design, *Energy and Buildings*, 307, 113991.

Khakre V.V., Wankhade A.M. (2014), Review paper on design and computational analysis of air flow through cooling duct, *International Journal of Scientific and Engineering Research*, 5(9), 123–128.

Liang R., Wang C., Wang P., Yoon S. (2023), Realization of rule-based automated design for HVAC duct layout, *Journal of Building Engineering*, 80, 107946.

Pacak A., Baran B., Sierpowski K., Malecha Z., Pandelidis D. (2023), Application of computational fluid dynamics (CFD) methods to analyze energy efficiency of indirect evaporative coolers, *International Communications in Heat and Mass Transfer*, 143, 106727.

Seuntjens O., Belmans B., Buyle M., Audenaert A. (2022), A critical review on the adaptability of ventilation systems: current problems, solutions and opportunities, *Building and Environment*, 212, 108816.

Su Z., Li X. (2022), Analysis of energy-saving for ventilation and air-conditioning system of subway stations with platform screen doors, *Journal of Building Engineering*, 59, 105064.

Walunj S., Shirasth S., Biradar A., Selvi A., Deore M. (2021), Study and analysis of air flow through duct, *Journal of Emerging Technologies and Innovative Research*, 8(6), 69–72.

Wang H., Zhu J., Dai Y., Hu H. (2023), A simplified cooling load calculation method based on equivalent heat transfer coefficient for large space buildings with a stratified air-conditioning system, *Energy and Buildings*, 296, 113370.

Wei W., Ramalho O., Mandin C. (2015), Indoor air quality requirements in green building certifications, *Building and Environment*, 92, 10–19.

Whalley R., Abdul-Ameer A. (2011), Heating, ventilation and air conditioning system modeling, *Building and Environment*, 46, 643–656.